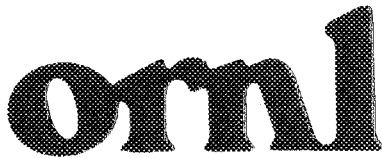


3 4456 0278653 6

ORNL/TM-10574



OAK RIDGE
NATIONAL
LABORATORY



Transport Scaling in the Collisionless-Detrapping Regime in Stellarators

E. C. Crume, Jr.
K. C. Shaing
S. P. Hirshman
W. I. van Rij

OAK RIDGE NATIONAL LABORATORY
CENTRAL RESEARCH LIBRARY
CIRCULATION SECTION
4009 YORK 125

LIBRARY LOAN COPY

DO NOT TRANSFER TO ANOTHER PERSON
If you wish someone else to see this
report, send in name with report and
the library will arrange a loan.

ORNL-10574

Printed in the United States of America. Available from
National Technical Information Service
U.S. Department of Commerce
5285 Port Royal Road, Springfield, Virginia 22161
NTIS price codes—Printed Copy: A02 Microfiche: A01

This report was prepared as an account of work sponsored by an agency of the United States Government. Neither the United States Government nor any agency thereof, nor any of their employees, makes any warranty, express or implied, or assumes any legal liability or responsibility for the accuracy, completeness, or usefulness of any information, apparatus, product, or process disclosed, or represents that its use would not infringe privately owned rights. Reference herein to any specific commercial product, process, or service by trade name, trademark, manufacturer, or otherwise, does not necessarily constitute or imply its endorsement, recommendation, or favoring by the United States Government or any agency thereof. The views and opinions of authors expressed herein do not necessarily state or reflect those of the United States Government or any agency thereof.

ORNL/TM-10574
Dist. Category UC-20 g

Fusion Energy Division

**TRANSPORT SCALING IN THE
COLLISIONLESS-DETRAPPING REGIME
IN STELLARATORS**

**E. C. Crume, Jr.
K. C. Shaing
S. P. Hirshman**

W. I. van Rij
Computing and Telecommunications Division,
Martin Marietta Energy Systems, Inc.

Date Published: September 1987

Prepared by the
OAK RIDGE NATIONAL LABORATORY
Oak Ridge, Tennessee 37831
operated by
MARTIN MARIETTA ENERGY SYSTEMS, INC.
for the
U.S. DEPARTMENT OF ENERGY
under contract DE-AC05-84OR21400



3 4456 0278653 6

ABSTRACT

Stellarator transport scalings with electric field, geometry, and collision frequency in the reactor-relevant collisionless-detraping regime are determined from numerical solutions of the drift kinetic equation. A new geometrical scaling, proportional to $\epsilon_t^{3/2}$ rather than $\epsilon_t \epsilon_h^{1/2}$, is found, where ϵ_t is the inverse aspect ratio and ϵ_h is the helical ripple. With the new scaling, no reduction in energy confinement time is associated with large helical ripple, which provides design flexibility. Integral expressions for the particle and heat fluxes that are useful for transport simulations are given.

Various scalings of stellarator transport have been obtained¹⁻⁴ in the low collisionality regime where $\nu_h \lesssim \Omega_E$. Here, $\nu_h = \nu/\epsilon_h$, ν is the collision frequency, ϵ_h the helical modulation of the magnetic field, and Ω_E the poloidal $\mathbf{E} \times \mathbf{B}$ drift frequency. We systematically investigate transport in this regime (also called the collisionless-detrapping regime, or the ν regime) using a comprehensive numerical treatment⁵ for analysis of neoclassical transport in general three-dimensional confinement geometries. The numerical calculations were carried out using a truncated stellarator magnetic field spectrum $B = B_0 [1 - \epsilon_t \cos \theta + \epsilon_h \cos(\ell\theta - m\zeta)]$, where B_0 is the magnetic field strength on axis, θ (ζ) is the poloidal (toroidal) angle, ϵ_t is the dominant toroidal magnetic field harmonic amplitude, and ℓ (m) is the poloidal (toroidal) mode number.

The fields used are representative of the vacuum magnetic fields of the Advanced Toroidal Facility (ATF),⁶ an $\ell = 2$, $m = 12$ torsatron. For ATF, the truncated spectrum is adequate for transport studies; we found only negligible differences when we repeated the calculations using a more complete, eight-term magnetic field spectrum. (However, a truncated spectrum would not be adequate for transport-optimized stellarators.^{7,8}) We find that the transport scaling in the collisionless-detrapping regime is essentially independent of ϵ_h but is proportional to $\epsilon_t^{3/2}$, where ϵ_t is the inverse aspect ratio. Previous results^{1,2} had shown an $\epsilon_h^{1/2} \epsilon_t$ dependence. Consequently, the penalty of reduced energy confinement time thought to be associated with large helical ripple is eliminated, allowing more flexibility in stellarator design. Finally, we have modified integral expressions⁹ for particle and heat fluxes in the low collisionality regime to reflect the new scaling.

The numerical treatment⁵ is embodied in the DKES (Drift Kinetic Equation Solver) code, which solves the linearized drift kinetic equation,

$$\mathbf{v} \cdot \nabla f_1 + \dot{\alpha}(\partial f_1 / \partial \alpha) - C(f_1) = S, \quad (1)$$

where f_1 is the deviation of the particle distribution from the Maxwellian f_M , $\mathbf{v} = v \cos \alpha \hat{n} + E_\rho \nabla \rho \times \hat{n} / \langle B^2 \rangle$, $\hat{n} = \mathbf{B}/B$, $v_{\parallel}/v = \cos \alpha$, $\dot{\alpha} = -(v/2)(\sin \alpha) \mathbf{B} \cdot \nabla(1/B)$, $S = f_M [-\mathbf{V}_d \cdot \nabla \rho (A_1 + x A_2) - B v \cos \alpha A_3]$, $A_1 = n'/n - 3T'/2T - eE_\rho/T$, $A_2 = T'/T$, $A_3 = -e \langle \mathbf{E} \cdot \mathbf{B} \rangle / T \langle B^2 \rangle$, $\mathbf{V}_d = -\hat{n} \times [e\mathbf{E} - (Mv_{\perp}^2/2)\nabla \ln B] / M\Omega + (v_{\parallel}^2/\Omega) \times [\nabla \times \hat{n} - (\hat{n} \cdot \nabla \times \hat{n})\hat{n}]$, $E_\rho = -d\Phi/d\rho$ with Φ the electrostatic potential, ρ is the radial flux coordinate, the angle brackets denote the flux-surface average, and $x = Mv^2/2T$. In obtaining Eq. (1), we neglect the $O(1/B)$ curvature and ∇B drift terms in $\mathbf{v} \cdot \nabla f_1$, so transport phenomena associated with resonant superbanana orbits¹⁰ are not treated. However, the poloidal $\mathbf{E} \times \mathbf{B}$ drift is included to calculate the effects of collisionless detrapping/retrapping of particles in helically trapped orbits. For these calculations, a pitch-angle scattering operator is used for $C(f_1)$.

The treatment here of the boundary layer between trapped and circulating particles is exact; therefore, no simplifying assumptions⁷ regarding boundary conditions on the distribution function are made. Equation (1) is solved in terms of Fourier-Legendre series for f_1 at a fixed value of normalized energy x for a number of values of ν and the electric field E_ρ . The thermodynamic fluxes I_i conjugate to the forces A_i can then be obtained from the appropriate moments of f_1 :

$$I_1 \equiv \langle \mathbf{\Gamma} \cdot \nabla \rho \rangle = \left\langle \int d^3v \mathbf{V}_d \cdot \nabla \rho f_1 \right\rangle = - \sum_{n=1}^2 L_{1n} A_n, \quad (2a)$$

$$I_2 \equiv \left\langle \frac{\mathbf{Q} \cdot \nabla \rho}{T} \right\rangle = \left\langle \int d^3v \mathbf{V}_d \cdot \nabla \rho x f_1 \right\rangle = - \sum_{n=1}^2 L_{2n} A_n, \quad (2b)$$

where $\mathbf{\Gamma}$ is the particle flux and \mathbf{Q} is the heat flux. [In Eq. (2) we ignore the contribution to the fluxes from A_3 .]

In Fig. 1(a) we show the plasma ion transport coefficient L_{22} versus ν/ω_{tr} on a vacuum flux surface of ATF. (Although we use the transport coefficient L_{22} in the examples, the same scalings are obtained from L_{11} and $L_{12} = L_{21}$.) Here $\omega_{\text{tr}} = v_T \langle B^\theta B^{-1} \rangle$ is the transit frequency, where $v_T = \sqrt{2T/M}$ is the thermal speed and B^θ is the contravariant θ component of \mathbf{B} . Curves are plotted for representative values of $e\Phi/T$, with the electric field scale length $\bar{a} = 30$ cm expected in ATF. Note that the transport coefficient L_{22} given here should be supplemented by the self-consistent determination of the electric field to obtain confinement times for a specific device.¹¹ In the low collisionality regime, where $\nu/\omega_{\text{tr}} < 10^{-3}$, the transport coefficient L_{22} is found to be proportional to $1/\Phi^2$. However, the transport scaling study is complicated by a resonance between the parallel streaming velocity v_{\parallel} and the poloidal $\mathbf{E} \times \mathbf{B}$ drift, which causes the transport scaling with respect to the electric field to deviate from $1/\Phi^2$, as it does in Fig. 1(b) for $e\Phi/T \gtrsim 5$. To obtain the transport scaling due to the effect of collisionless detrapping/retrapping, we have carefully avoided this resonance by examining the Φ scaling for each set of parameters using the type of plot shown in Fig. 1. If the Φ scaling deviates from $1/\Phi^2$, this usually implies a resonance for a nearby value of the electric field. The results near such a resonance are not used in determining the present scaling.

In Fig. 2, the normalized transport coefficient $L_{22}\Omega_E/\Omega_{E0}$ is plotted versus ν_h/Ω_E for several values of E_ρ at fixed ϵ_t and ϵ_h . From this figure, we conclude that L_{22} is linearly proportional to ν , in contrast to the $\nu^{3/4}$ scaling obtained in Ref. 3. Clearly, the $1/\Omega_E^2 \propto 1/\Phi^2$ scaling for L_{22} is also confirmed. For a given value of $e\Phi/T$, we have varied ϵ_t from 0.029 to 0.232 and ϵ_h from 0.035 to 0.283. The results are presented in Fig. 3, which shows the normalized transport coefficient $\epsilon_t^{-3/2} L_{22}/L_{22}^0$ versus ϵ_h , where $L_{22}^0 = L_{22}(\epsilon_t = 0.12, \epsilon_h = 0.14)$. It is seen that $\epsilon_t^{-3/2} L_{22}/L_{22}^0$ is not very sensitive to the value of ϵ_h . Consequently, the dominant geometric dependence of L_{22} is $\epsilon_t^{3/2}$. From the results shown in Figs. 1–3,

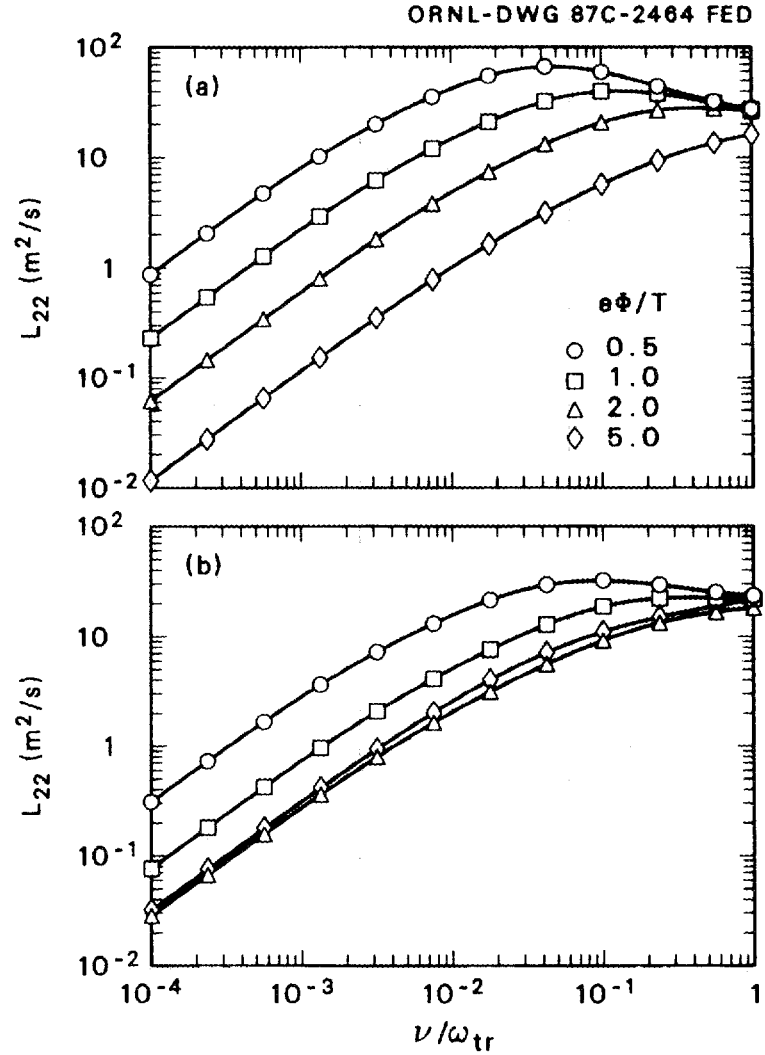


Fig. 1. Transport coefficient L_{22} versus ν/ω_{tr} for two flux surfaces of a model ATF-like torsatron with $\ell = 2$, $m = 12$. (a) $\epsilon_t = 0.12$, $\epsilon_h = 0.14$, $\tau = 0.68$. (b) $\epsilon_t = 0.071$, $\epsilon_h = 0.066$, $\tau = 0.45$. Here, τ is the rotational transform.

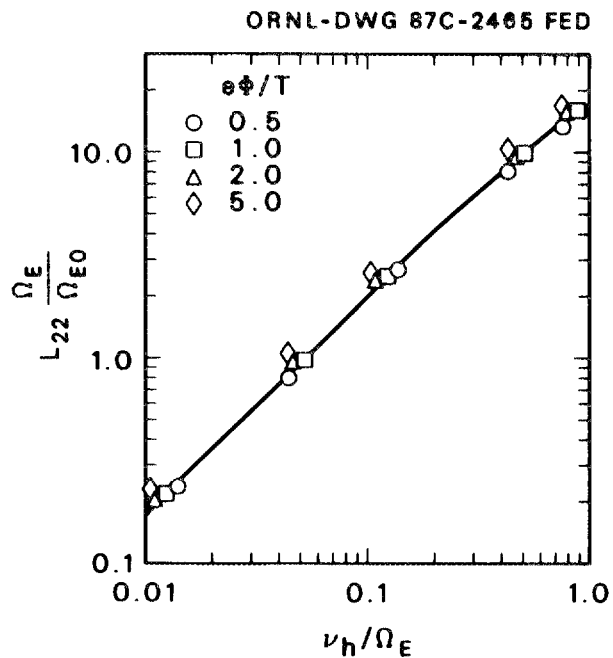


Fig. 2. Electric field and collision frequency scaling for transport in the collisionless-detrapping regime (ν regime). $\Omega_{E0} = \Omega_E(e\Phi/T = 1)$.

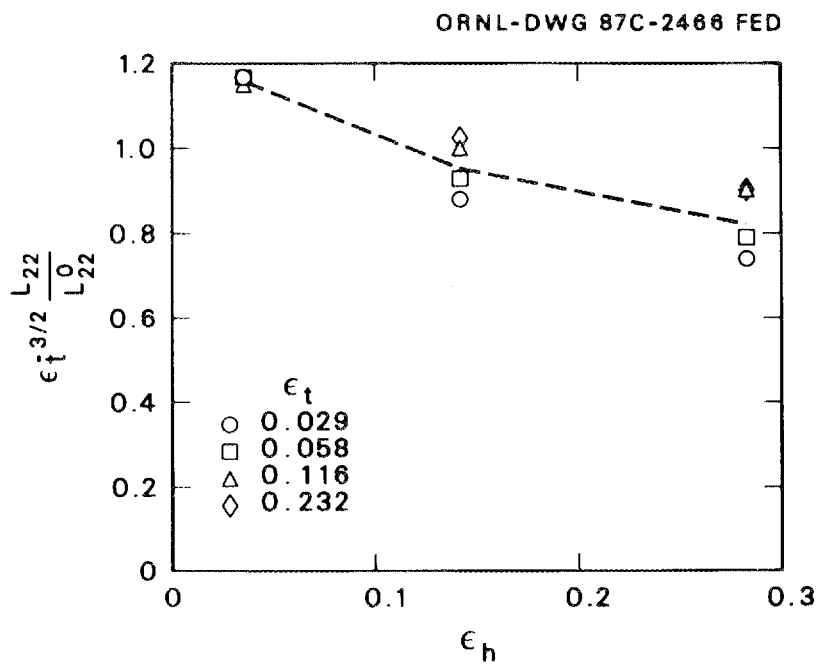


Fig. 3. Geometrical scaling for transport in the collisionless-detrapping regime (ν regime). $L_{22}^0 = L_{22}(\epsilon_t = 0.12, \epsilon_h = 0.14)$.

we conclude that the transport scaling due to collisionless detrapping/retrapping orbits is $L_{22}^{\text{DKES}} \propto \nu \epsilon_t^{3/2} / \Omega_E^2$. This scaling differs from that in Refs. 1 and 2, where $L_{22}^{\text{GS}} \propto \nu \epsilon_t \sqrt{\epsilon_h} / \Omega_E^2$ was obtained.

The scaling we have found for L_{22}^{DKES} can be understood heuristically from a random walk argument. In the ν regime, the step size Δr is determined by the helically trapped particles and is $\Delta r \simeq V_d / \Omega_E \cong \epsilon_t T / (M \Omega r \Omega_E)$, where $V_d = \epsilon_t T / (M \Omega r)$ is the radial drift velocity and r is the local minor radius. The diffusion coefficient $D \sim f(\Delta r)^2 / \Delta t \sim \nu(\Delta r)^2 / f$, where $\Delta t \sim (\nu / f^2)^{-1}$ is assumed and f is the fraction of particles that participate in the transport process. The scaling obtained from the DKES results indicates that $f \sim \sqrt{\epsilon_t} G^{-1}(\epsilon_h, \epsilon_t)$, where G is a weak function of ϵ_h and ϵ_t . Thus, since $L \propto D$, we find $L^{\text{DKES}} \sim \nu \epsilon_t^{3/2} G(\epsilon_h, \epsilon_t) T^2 / (M^2 \Omega^2 r^2 \Omega_E^2)$.

The DKES numerical results for the collisionless-detrapping regime are incorporated into the smoothly connected integral expressions given in Ref. 9 for the particle flux Γ_a and the heat flux Q_a of charged particle species,

$$\begin{bmatrix} \Gamma_a \\ Q_a \end{bmatrix} = -\epsilon_t^2 \sqrt{\epsilon_h} v_a^2 \begin{bmatrix} n_a \\ n_a T_a \end{bmatrix} \int_b^\infty dx_a \begin{bmatrix} x_a^{5/2} \\ x_a^{7/2} \end{bmatrix} \exp(-x_a) \frac{\nu_{ah}(x_a)(A_{a1} + x_a A_{a2})}{\omega_a^2(x_a)}, \quad (3)$$

where $v_a = V_{da} / \epsilon_t$, $\nu_{ah}(x_a) = \nu_{ii}(x_i) / \epsilon_h$ for ions and $\nu_{ah}(x_a) = [\nu_{ee}(x_e) + \nu_{ei}(x_e)] / \epsilon_h$ for electrons, and $b = [\nu_{ah}(1) R / v_{Ta} m \epsilon_h^{1/2}]^{1/2}$ is the smallest value of x_a for which particles have effective collision frequencies smaller than their bounce frequency in a helical well. Here, R is the major radius of the flux surface and v_{Ta} is the thermal speed of species a . For this problem, where the ∇B drift term has not been included in $\mathbf{v} \cdot \nabla f_1$,

$$\omega_a^2(x_a) = 1.5 \sqrt{\epsilon_t / \epsilon_h} \Omega_E^2 + 3\nu_{ah}^2(x_a), \quad (4)$$

where the first term on the right is the dominant term in the collisionless-detrapping regime and the second term is the dominant term in the $1/\nu$ regime. In Ref. 9, $\omega_a^2 = 1.67 \epsilon_t / \epsilon_h \Omega_E^2 + 3\nu_{ah}^2(x_a)$, which gives the same geometrical scaling in the collisionless-detrapping regime as that in Refs. 1 and 2, $L_{22} \propto \epsilon_t \epsilon_h^{1/2}$. In Fig. 4, we plot L_{22} versus ν / ω_{tr} for two ratios of ϵ_t / ϵ_h at fixed ϵ_h ; the solid curves are DKES results and the dash-dot curves come from numerical integration of Eq. (3). As would be expected, the agreement is very good for $\nu / \omega_{tr} \lesssim 10^{-2}$. For larger ν / ω_{tr} , the DKES results are always higher because the plateau-Pfirsch-Schlüter contributions have been ignored in Eq. (3). Also in Fig. 4, we plot L_{22}^{GS} (dashed lines) for both ϵ_t / ϵ_h ratios. As expected from the earlier discussion, L_{22}^{GS} shows the same collision frequency scaling as L_{22}^{DKES} ; the differences in geometrical scaling result from the different ϵ_t dependences.

Recently, a theory for stellarator transport valid in all low collisionality regimes was proposed.⁷ We find that this theory does not yield a collision frequency scaling proportional to the first power of ν in the collisionless-detrapping regime, even

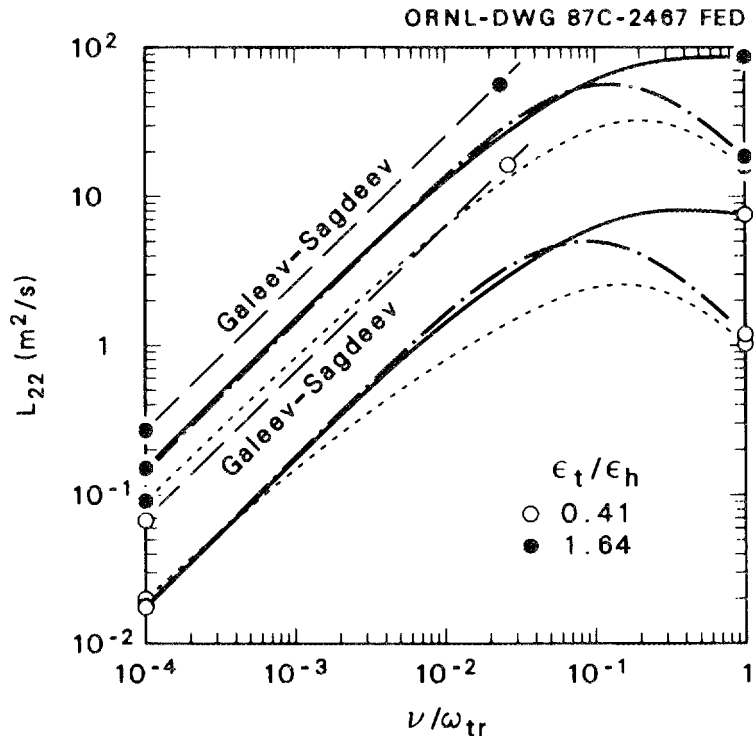


Fig. 4. Comparison of L_{22} scalings with DKES results for two ϵ_t/ϵ_h ratios. Solid curves: DKES results; dash-dot curves: this paper; long-dash curves: Galeev-Sagdeev scaling; short-dash curves: Beidler et al. scaling.

though it is derived from an equation similar to Eq. (1). This is illustrated in Fig. 4, where $L_{22}^{\text{Ref. 7}}$ is plotted (dotted curves) for the ϵ_t/ϵ_h ratios. We have not included the purely axisymmetric contribution to the Ref. 7 transport coefficient so that the overall differences in the scalings can be better illustrated. The deviation from the ν scaling is less for the higher value of ϵ_t/ϵ_h but is still obvious in comparison with the nearby L_{22}^{GS} curve. For $\nu/\omega_{\text{tr}} \lesssim 10^{-2}$, although the numerical results of Ref. 7 are within a factor of 2 of our results or better for the cases illustrated, differences in both the collision frequency and geometrical scalings are apparent.

The transport scaling for the diffusion coefficients in stellarator devices has been studied using a numerical treatment incorporated into the DKES code. In the collisionless-detraping regime, the scaling differs from previous scalings obtained with various analytic and other numerical treatments. The discrepancies probably result from approximate boundary conditions imposed in the other treatments at the boundaries between helically trapped and toroidally trapped particles; no such conditions are imposed here. The primary consequence of the new scaling is to allow more flexibility in stellarator design, since the magnitude of the helical ripple does not enter into the transport scaling.

ACKNOWLEDGMENTS

The authors are grateful to J. A. Rome for providing the spectra of the ATF magnetic field and to W. A. Houlberg for a computer program to calculate the L_{ij} from Eq. (3).

REFERENCES

- ¹A. A. Galeev and R. Z. Sagdeev, *Usp. Fiz. Nauk.* **99**, 528 (1969) [*Sov. Phys. Usp.* **14**, 810 (1969)].
- ²H. E. Mynick, *Phys. Fluids* **26**, 2609 (1983).
- ³L. M. Kovrizhnykh, *Nucl. Fusion* **24**, 851 (1984).
- ⁴K. C. Shaing, J. A. Rome, and R. H. Fowler, *Phys. Fluids* **27**, 1 (1984).
- ⁵S. P. Hirshman, K. C. Shaing, W. I. van Rij, C. O. Beasley, Jr., and E. C. Crume, Jr., *Phys. Fluids* **29**, 2951 (1986).
- ⁶J. F. Lyon, B. A. Carreras, K. K. Chipley, M. J. Cole, J. H. Harris, T. C. Jernigan, R. L. Johnson, V. E. Lynch, B. E. Nelson, J. A. Rome, J. Sheffield, and P. B. Thompson, *Fusion Technol.* **10**, 179 (1986).
- ⁷C. D. Beidler, W.N.G. Hitchon, W. I. van Rij, S. P. Hirshman, and J. L. Shohet, *Phys. Rev. Lett.* **58**, 1745 (1987).
- ⁸H. E. Mynick, T. K. Chu, and A. H. Boozer, *Phys. Rev. Lett.* **48**, 322 (1982).
- ⁹K. C. Shaing, *Phys. Fluids* **27**, 1567 (1984).
- ¹⁰A. A. Galeev, R. Z. Sagdeev, H. P. Furth, and M. N. Rosenbluth, *Phys. Rev. Lett.* **22**, 511 (1969).
- ¹¹D. E. Hastings, W. A. Houlberg, and K. C. Shaing, *Nucl. Fusion* **25**, 445 (1985).

INTERNAL DISTRIBUTION

- | | | | |
|--------|------------------|--------|---|
| 1. | C. O. Beasley | 22. | J. F. Lyon |
| 2. | B. A. Carreras | 23. | J. A. Rome |
| 3-7. | E. C. Crume, Jr. | 24-28. | K. C. Shaing |
| 8. | N. Dominguez | 29-33. | W. I. van Rij |
| 9. | R. A. Dory | 34. | J. Sheffield |
| 10. | J. L. Dunlap | 35-36. | Laboratory Records Department |
| 11. | R. H. Fowler | 37. | Laboratory Records, ORNL-RC |
| 12. | J. H. Harris | 38. | Central Research Library |
| 13. | C. L. Hedrick | 39. | Document Reference Section |
| 14-18. | S. P. Hirshman | 40. | Fusion Energy Division Library |
| 19. | W. A. Houlberg | 41-42. | Fusion Energy Division
Publications Office |
| 20. | H. C. Howe | 43. | ORNL Patent Office |
| 21. | R. C. Isler | | |

EXTERNAL DISTRIBUTION

44. Office of the Assistant Manager for Energy Research and Development, U.S. Department of Energy, Oak Ridge Operations Office, P. O. Box E, Oak Ridge, TN 37831
45. J. D. Callen, Department of Nuclear Engineering, University of Wisconsin, Madison, WI 53706-1687
46. J. F. Clarke, Director, Office of Fusion Energy, Office of Energy Research, ER-50 Germantown, U.S. Department of Energy, Washington, DC 20545
47. R. W. Conn, Department of Chemical, Nuclear, and Thermal Engineering, University of California, Los Angeles, CA 90024
48. S. O. Dean, Fusion Power Associates, Inc., 2 Professional Drive, Suite 249, Gaithersburg, MD 20760
49. H. K. Forsen, Bechtel Group, Inc., Research Engineering, P. O. Box 3965, San Francisco, CA 94105
50. J. R. Gilleland, GA Technologies, Inc., Fusion and Advanced Technology, P.O. Box 85608, San Diego, CA 92138
51. R. W. Gould, Department of Applied Physics, California Institute of Technology, Pasadena, CA 91125
52. R. A. Gross, Plasma Research Laboratory, Columbia University, New York, NY 10027

53. D. M. Meade, Princeton Plasma Physics Laboratory, P.O. Box 451, Princeton, NJ 08544
54. M. Roberts, International Programs, Office of Fusion Energy, Office of Energy Research, ER-52 Germantown, U.S. Department of Energy, Washington, DC 20545
55. W. M. Stacey, School of Nuclear Engineering and Health Physics, Georgia Institute of Technology, Atlanta, GA 30332
56. D. Steiner, Nuclear Engineering Department, NES Building, Tibbetts Avenue, Rensselaer Polytechnic Institute, Troy, NY 12181
57. R. Varma, Physical Research Laboratory, Navrangpura, Ahmedabad 380009, India
58. Bibliothek, Max-Planck Institut für Plasmaphysik, Boltzmannstrasse 2, D-8046 Garching, Federal Republic of Germany
59. Bibliothek, Institut für Plasmaphysik, KFA Jülich GmbH, Postfach 1913, D-5170 Jülich, Federal Republic of Germany
60. Bibliothek, KfK Karlsruhe GmbH, Postfach 3640, D-7500 Karlsruhe 1, Federal Republic of Germany
61. Bibliothèque, Centre de Recherches en Physique des Plasmas, Ecole Polytechnique Fédérale de Lausanne, 21 Avenue des Bains, CH-1007 Lausanne, Switzerland
62. F. Prevot, CEN/Cadarache, Département de Recherches sur la Fusion Contrôlée, F-13108 Saint-Paul-lez-Durance Cedex, France
63. Bibliothèque, CEN/Cadarache, F-13108 Saint-Paul-lez-Durance Cedex, France
64. Library, Culham Laboratory, UKAEA, Abingdon, Oxfordshire, OX14 3DB, England
65. Library, JET Joint Undertaking, Abingdon, Oxfordshire OX14 3EA, England
66. Library, FOM-Instituut voor Plasmafysica, Rijnhuizen, Edisonbaan 14, 3439 MN Nieuwegein, The Netherlands
67. Library, Institute of Plasma Physics, Nagoya University, Chikusa-ku, Nagoya 464, Japan
68. Library, International Centre for Theoretical Physics, P.O. Box 586, I-34100 Trieste, Italy
69. Library, Centro Ricerca Energia Frascati, C.P. 65, I-00044 Frascati, Rome, Italy
70. Library, Plasma Physics Laboratory, Kyoto University, Gokasho, Uji, Kyoto, Japan
71. Plasma Research Laboratory, Australian National University, P.O. Box 4, Canberra, A.C.T. 2000, Australia
72. Library, Japan Atomic Energy Research Institute, Naka-machi, Nakagun, Ibaraki-ken 311-02, Japan

73. Library, Japan Atomic Energy Research Institute, Mukouyama, Nakamachi, Naka-gun, Ibaraki-ken, 311-02 Japan
74. G. A. Eliseev, I. V. Kurchatov Institute of Atomic Energy, P. O. Box 3402, 123182 Moscow, U.S.S.R.
75. V. A. Glukhikh, Scientific-Research Institute of Electro-Physical Apparatus, 188631 Leningrad, U.S.S.R.
76. I. Shpigel, Institute of General Physics, U.S.S.R. Academy of Sciences, Ulitsa Vavilova 38, Moscow, U.S.S.R.
77. D. D. Ryutov, Institute of Nuclear Physics, Siberian Branch of the Academy of Sciences of the U.S.S.R., Sovetskaya St. 5, 630090 Novosibirsk, U.S.S.R.
78. V. T. Tolok, Kharkov Physical-Technical Institute, Academical St. 1, 310108 Kharkov, U.S.S.R.
79. Library, Academia Sinica, P.O. Box 3908, Beijing, China (PRC)
80. R. A. Blanken, Experimental Plasma Research Branch, Division of Applied Plasma Physics, Office of Fusion Energy, Office of Energy Research, ER-542, Germantown, U.S. Department of Energy, Washington, DC 20545
81. K. Bol, Princeton Plasma Physics Laboratory, P.O. Box 451, Princeton, NJ 08544
82. R. A. E. Bolton, IREQ Hydro-Quebec Research Institute, 1800 Montee Ste.-Julie, Varennes, P.Q. JOL 2P0, Canada
83. D. H. Crandall, Experimental Plasma Research Branch, Division of Applied Plasma Physics, Office of Fusion Energy, Office of Energy Research, ER-542, Germantown, U.S. Department of Energy, Washington, DC 20545
84. R. L. Freeman, GA Technologies, Inc., P.O. Box 85608, San Diego, CA 92138
85. K. W. Gentle, RLM 11.222, Institute for Fusion Studies, University of Texas, Austin, TX 78712
86. R. J. Goldston, Princeton Plasma Physics Laboratory, P.O. Box 451, Princeton, NJ 08544
87. J. C. Hosea, Princeton Plasma Physics Laboratory, P.O. Box 451, Princeton, NJ 08544
88. S. W. Luke, Division of Confinement Systems, Office of Fusion Energy, Office of Energy Research, ER-55, Germantown, U.S. Department of Energy, Washington, DC 20545
89. E. Oktay, Division of Confinement Systems, Office of Fusion Energy, Office of Energy Research, ER-55, Germantown, U.S. Department of Energy, Washington, DC 20545
90. D. Overskei, GA Technologies, Inc., P.O. Box 85608, San Diego, CA 92138

91. R. R. Parker, Plasma Fusion Center, NW 16-288, Massachusetts Institute of Technology, Cambridge, MA 02139
92. W. L. Sadowski, Fusion Theory and Computer Services Branch, Division of Applied Plasma Physics, Office of Fusion Energy, Office of Energy Research, ER-541, Germantown, U.S. Department of Energy, Washington, DC 20545
93. J. W. Willis, Division of Confinement Systems, Office of Fusion Energy, Office of Energy Research, ER-55, Germantown, U.S. Department of Energy, Washington, DC 20545
94. A. P. Navarro, Division de Fusion, CIEMAT, Avenida Complutense 22, E-28040 Madrid, Spain
95. Laboratory for Plasma and Fusion Studies, Department of Nuclear Engineering, Seoul National University, Shinrim-dong, Gwanak-ku, Seoul 151, Korea
96. J. L. Johnson, Plasma Physics Laboratory, Princeton University, P.O. Box 451, Princeton, NJ 08544
97. L. M. Kovrizhnykh, Institute of General Physics, U.S.S.R. Academy of Sciences, Ulitsa Vavilova 38, 117924 Moscow, U.S.S.R.
98. O. Motojima, Plasma Physics Laboratory, Kyoto University, Gokasho, Uji, Kyoto, Japan
99. V. D. Shafranov, I. V. Kurchatov Institute of Atomic Energy, P.O. Box 3402, 123182 Moscow, U.S.S.R.
100. J. L. Shohet, Torsatron/Stellarator Laboratory, University of Wisconsin, Madison, WI 53706
101. H. Wobig, Max-Planck Institut für Plasmaphysik, D-8046 Garching, Federal Republic of Germany
102. C. D. Beidler, Torsatron/Stellarator Laboratory, University of Wisconsin, Madison WI 53706
103. W. N. G. Hitchon, Torsatron/Stellarator Laboratory, University of Wisconsin, Madison WI 53706
104. H. Mynick, Princeton Plasma Physics Laboratory, Princeton, NJ 08544
105. H. Maassberg, Max-Planck-Institut für Plasmaphysik, Boltzmanstrasse 2, D-8046 Garching, Federal Republic of Germany
- 106-221. Given distribution as shown in TIC-4500, Magnetic Fusion Energy (Distribution Category UC-20 g: Theoretical Plasma Physics)